Contemporary Mathematics
https://ojs.wiserpub.com/index.php/CM/

Research Article

Optimizing Air Photovoltaic/Thermal Solar Collectors: Integrating a Fuzzy Logic Approach for Enhanced Efficiency

Noran Nur Wahida Khalili[1*], Rajalingam Sokkalingam[2], Mahmod Othman[3], Muhammad Naeim Mohd Aris[4]

[1]Maritime Management Section, Malaysian Institute of Marine Engineering Technology, Universiti Kuala Lumpur, 32000, Lumut, Perak, Malaysia
[2]Fundamental and Applied Sciences Department, Universiti Teknologi PETRONAS, 32610, Seri Iskandar, Perak, Malaysia
[3]Department of Information System, Universitas Islam Indragiri, Tembilahan Hulu, 29213, Indonesia
[4]Department of Mathematical Sciences, Faculty of Science and Technology, Universiti Kebangsaan Malaysia, 43600, Bangi, Selangor, Malaysia
E-mail: nwahidakhalili04@unikl.edu.my

Received: 16 December 2024; **Revised:** 15 February 2025; **Accepted:** 28 April 2025

Abstract: The increasing global energy demand necessitates improvements in renewable energy efficiency, particularly in solar energy systems. This study aims to develop a compact Photovoltaic/Thermal (PV/T) solar collector using air as the working fluid, designed to achieve higher efficiency and better space utilization compared to traditional systems. The performance of PV/T collectors is influenced by environmental factors such as solar intensity and ambient temperature, posing challenges in determining the optimal air mass flow rate. To address this, a fuzzy logic-based automated control system is developed, integrating a Weighted Subsethood-based algorithm and Fuzzy Subjective Evaluation, to dynamically optimize fan speed under varying conditions. This study highlights the importance of adaptive control in renewable energy systems and offers a scalable, transportable solution for maximizing solar energy utilization. This approach maintains the balance between input and output energy, demonstrating that the highest air mass flow rate is not always necessary for optimal performance.

***Keywords*:** fuzzy optimization, photovoltaic/thermal, solar collector, mathematical model

MSC: 93C42, 94D05, 90C70

1. Introduction

Solar energy, being a clean and limitless resource, has emerged as a key component of global attempts to shift to sustainable energy systems. With the growing desire for renewable energy sources to combat climate change and reduce reliance on fossil fuels, solar energy has gained traction due to its ubiquitous availability and low cost. Over the last decade, solar energy's economic feasibility has increased considerably. For example, the global average cost of generating one megawatt-hour of power from solar Photovoltaic (PV) sources has decreased, making it more cost-effective than nuclear and coal and competitive with onshore wind energy [1], as shown in Figure 1. This cost reduction, combined with advances in solar technology, has established solar energy as a prominent participant in the global energy scene.

DOI: https://doi.org/10.37256/cm.6420256250

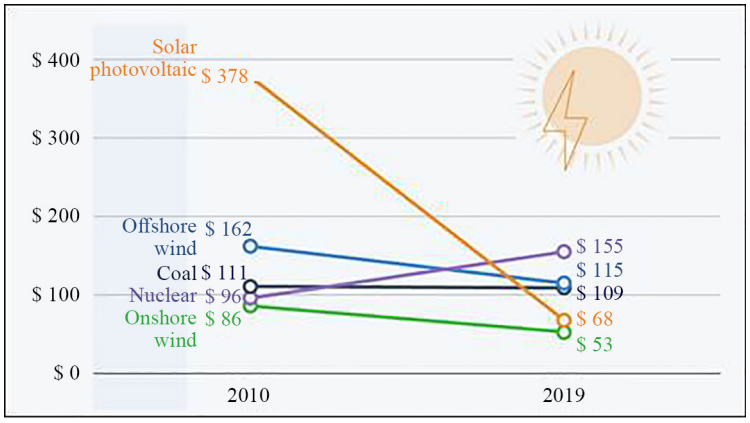

Figure 1. Global weighted average of levelized costs of energy, price per megawatt hour of electricity [1]

Solar energy can be harnessed through various technologies, including Photovoltaic (PV) collectors, Thermal (T) solar collectors, and hybrid Photovoltaic/Thermal (PV/T) systems. PV collectors directly convert solar energy into electricity, whereas thermal collectors gather heat for use in space or water heating. Hybrid PV/T systems integrate both technologies to generate energy while also using waste heat from PV panels, enhancing total system efficiency.

Advancements in thermal storage have been significant studies in enhancing the efficiency and reliability of solar energy systems. A thorough analysis of Phase Change Materials (PCMs) emphasised their ability to store huge amounts of energy during phase transitions, which considerably increases the thermal efficiency of PV/T systems [2]. A research [3] has investigated sensible heat storage materials such as water, rocks, and concrete, emphasising their economic viability and broad use in sun thermal applications. Thermochemical storage systems, which store energy via reversible chemical reactions while providing high energy density and long-term storage capabilities has been studied in [4]. Researchers in [5] investigated the use of nanoparticles to improve the thermal conductivity of PCMs, resulting in faster heat absorption and release in thermal storage devices.

The inverse relationship between thermal energy generation and photovoltaic efficiency, on the other hand, is a difficulty for PV/T systems. As the temperature of solar cells rises due to heat accumulation, their electrical efficiency falls dramatically. To overcome this, working fluid, such as water or air, is used to cool the PV module, increasing electrical output while also absorbing thermal energy for secondary purposes [6]. Air is commonly opted for over other cooling fluids because of its simplicity, availability, and low maintenance requirements. Unlike water-based systems, air-cooled PV/T systems do not require sophisticated infrastructure, are less prone to freezing or leakage, and do not pose the same safety risks as high-temperature fluids. Table 1 below shows the summary of air-based PV/T systems in previous work, focusing on the systems description, advantages and disadvantages and their applications.

However, the efficiency of air-based PV/T systems is heavily reliant on the efficient control of air mass flow rates, which are impacted by dynamic environmental parameters such as solar irradiation, ambient temperature, and wind velocity. Traditional control approaches, which rely on manual changes or simple automation, are frequently insufficient for optimising performance under changing conditions. This limitation emphasises an important research gap, which is the need for control systems that can automatically react to environmental changes in order to maximise electrical and thermal efficiency.

A promising solution to this problem is fuzzy logic, a computational framework for dealing with uncertainty and imprecision. Unlike traditional control systems that rely on exact mathematical models, fuzzy logic works with approximate reasoning and linguistic variables, which makes it ideal for complex, non-linear systems like PV/T collectors. By integrating fuzzy logic into the control mechanism, air mass flow rates can be optimised in real-time, resulting in effective heat removal and improved system performance [12, 13]. Despite its potential, the use of fuzzy logic in air-based PV/T systems is still understudied, especially when it comes to integrating weighted subsethood-based algorithms for decision-making.

Table 1. Summary of air-based PV/T systems in previous work

Ref.	System description	Advantages	Disadvantages	Applications
[7]	Air-based PV/T system with a flatplate collector and natural airflow	- Low cost - Simple design - No risk of leakage or freezing	- Lower thermal efficiency compared to liquid-based systems	Residential heating and drying applications
[8]	Air-based PV/T system with a double-pass airflow design for improved heat extraction	- Higher thermal efficiency - Better heat transfer	- Increased complexity and cost	Industrial process heating
[9]	Air-based PV/T system with a finned absorber plate to enhance heat transfer	- Improved thermal performance - Compact design	-Higher manufacturing cost	Small-scale residential and agricultural use
[10]	Air-based PV/T system with a focus on optimizing airflow rate for efficiency	- Enhanced electrical and thermal output - Easy maintenance	-Sensitive to environmental conditions (e.g.wind speed)	Greenhouses and space heating
[11]	Air-based PV/T system integrated with building structures (BIPV/T)	-Dual purpose (energy generation and building integration)	-Requires careful design and installation	Building-integrated renewable energy systems

This study addresses these gaps by developing an air-based PV/T solar collector model that incorporates a fuzzy logic control system to optimize air mass flow rates. The proposed system utilizes a fan to create forced airflow, with the fuzzy logic controller dynamically adjusting the fan speed based on real-time environmental data. The integration of a weighted subsethood-based algorithm further enhances the system's ability to handle uncertainty and imprecision, ensuring robust performance under varying conditions. By automating the control process, this research eliminates the subjectivity and inefficiencies associated with manual adjustments, offering a more reliable and adaptive solution for optimizing PV/T systems.

The importance of this study is in its ability to improve the viability and efficiency of air-based PV/T systems. This work presents a completely automated, fuzzy logic-based methodology that greatly increases system adaptability and energy output, whereas other research has concentrated on human or semi-automated control methods. Furthermore, the development of mathematical model and methodology for performance analysis offers important new perspectives on how PV/T systems behave in practical settings. This study leads to more sustainable and effective solar energy systems that may satisfy the rising demands of a future powered by renewable energy by addressing the shortcomings of current control techniques and utilising fuzzy logic's advantages.

2. Methodology

In this research, a fuzzy logic control system is implemented by firstly fuzzifying three environmental variables, which are solar irradiance, ambient temperature, and wind speed into fuzzy categories using triangular and trapezoidal fuzzy function. The system then employed a weighted subsethood method to create rules connecting these inputs to control outputs, which is the fan speed adjustments. Lastly, the system converts these fuzzy decisions into specific numerical values using the centroid technique for balanced output. This structured approach allows the system to respond effectively to changing environmental conditions while maintaining optimal performance.

2.1 *Fuzzy rules generation using weighted subsethood-based algorithm*

The weighted subsethood algorithm was chosen for generating rules, as it offers distinct benefits compared to other methods like traditional rule-based systems, genetic algorithms, and neural networks. The implementation of fuzzy logic

is particularly effective at managing imprecise environmental data [12]. While conventional rule-based systems use strict boundaries, the weighted subsethood algorithm employs fuzzy sets to handle overlapping states, for instance, when solar irradiance transitions between medium and high levels. This approach offers superior computational efficiency compared to genetic algorithms and neural networks, making it ideal for real-time control where quick responses are essential [13]. Additionally, unlike neural networks' "black box" nature, the weighted subsethood algorithm produces transparent, interpretable rules that can be easily modified and monitored [14]. These characteristics-efficiency, adaptability, and transparency-make the weighted subsethood algorithm an optimal choice that addresses the limitations of alternative optimization techniques.

In this study, the output is categorized into three clusters, which aligns with established PV/T system research, where environmental parameters are typically divided into low, medium, and high ranges to streamline control approaches and enhance system response times [8, 10]. This three-cluster structure shows an optimal balance, providing sufficient computational simplicity while maintaining the precise control needed for PV/T collectors to operate effectively across different environmental conditions.

This section illustrates the generation of fuzzy rules using a weighted subsethood-based algorithm. The experimental dataset contains 140 data points. The dataset is divided into training and testing subsets. The process of data splitting is elaborated in the following steps. In the context of this study, rules are generated according to the general Mamdani fuzzy laws [14], following the methodology outlined in [13, 15].

Step 1: The training data are clustered into three different clusters, referred to as Low, Medium, and High, using k-means clustering method. It should be noted that the clustering computation is performed using MATLAB software. To demonstrate *k*-means clustering, this example uses total efficiency data, as shown in Figure 2.

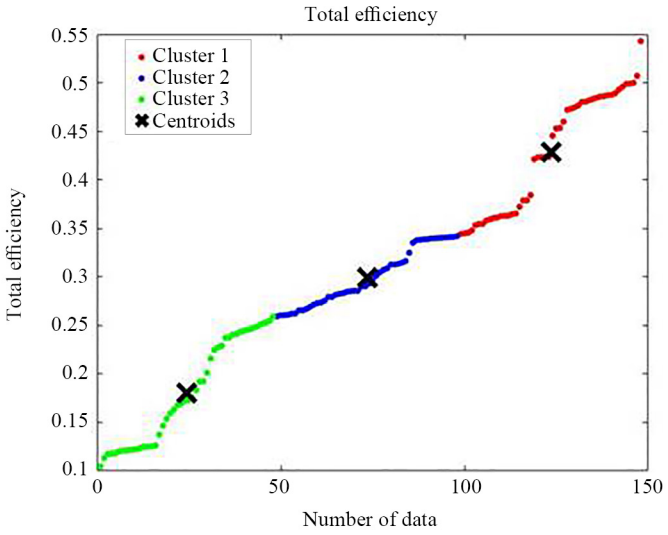

Figure 2. The clustering of total efficiency data into three clusters

Membership functions are then specifically generated for the inputs (solar radiation, ambient, temperature, air mass flow) and output (total efficiency) based on the clusters and their limits.

The result showed that total efficiency of less than 0.1076 or 10.76% is clustered as Cluster 1 (Low). Total efficiency that is between 0.1076 and 0.2995 is clustered as Cluster 2 (Medium). The remaining data are clustered as Cluster 3 (High). Table 2 presents the membership function values of the input and output parameters, and Figure 3 illustrates the membership function of solar radiation for those three different clusters.

Table 2. Membership functions of input and output variables

	Low	Medium	High
Total efficiency	0.181	0.299	0.429
Solar radiation $\left(\mathrm{W}\cdot\mathrm{m}^{-2}\right)$	162.222	371.875	753.521
Ambient temperature (K)	302.864	306.013	308.854
Air mass flow rate $\left(\mathrm{kg}\cdot\mathrm{s}^{-1}\right)$	0.011574	0.017802	0.035759

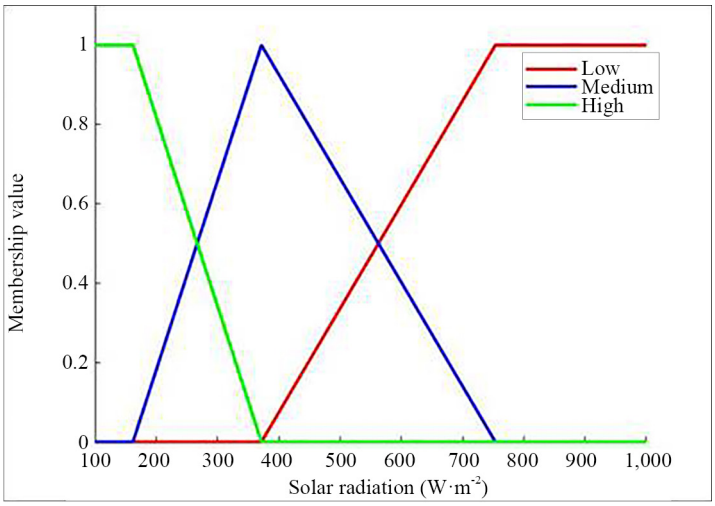

Figure 3. Membership function of solar radiation

The membership functions, μ, for solar radiation, G, for all clusters (Low, Medium and High) are as follows:

$$\mu_{\text{Low}}(G)=\begin{cases}1, & G<162.222\\ \dfrac{371.875-G}{371.875-162.222}, & 162.222<G<371.875\\ 0, & G\geq 371.875\end{cases} \tag{1}$$

$$\mu_{\text{Medium}}(G)=\begin{cases}0, & G<162.222\\ \dfrac{G-162.222}{371.875-162.222}, & 162.222<G<371.875\\ \dfrac{753.521-G}{753.521-371.8757}, & 371.8757<G\leq 753.521\\ 0, & G\geq 753.521\end{cases} \tag{2}$$

$$\mu_{\text{High}}(G) = \begin{cases} 0, & G < 371.875 \\ \dfrac{G - 371.8757}{753.521 - 371.8757}, & 371.8757 < G \leq 753.521 \\ 1, & G \geq 753.521 \end{cases} \tag{3}$$

Step 2: The training dataset consists of 70 data points, which is 50% of the overall dataset, divided equally by even and odd numbering in the list. The training dataset is used to develop fuzzy rules while testing dataset is later used to validate the fuzzy rules developed. The training dataset is arranged numerically and pre-processed where any repeated values are removed. The data in the training dataset is referred to as "data point", which is partly illustrated in Table 3. Next, all data points in the training dataset are then categorized into classification outcome based on the membership functions generated for total efficiency.

Table 3. Training dataset of ten data points based on clusters

Data point	Solar radiation ($W \cdot m^{-2}$)	Ambient temperature (K)	Air mass flowrate ($kg \cdot s^{-1}$)	Total efficiency	Outcome
1	900	308	0.046425	0.542934	High
2	200	306	0.038653	0.378829	Medium
3	600	303	0.037629	0.485978	High
4	300	303	0.037333	0.423715	High
5	700	306	0.036721	0.492894	High
6	400	304	0.036464	0.452913	High
7	200	306	0.036453	0.372299	Medium
8	400	305	0.036125	0.453442	High
9	900	307	0.035899	0.499143	High
10	200	305	0.035501	0.364717	Medium

Step 3: Referring to the classification outcomes of the total efficiency, tabulated in step 2, 70 data points in the training dataset are divided into three subgroups. Data points 23, 30, 43, 53, 58, 65-70 are classified in Subgroup 1 as low level of total efficiency, while data points 2, 7, 10, 12, 18, 19, 22, 24-29, 31-42, 44-52, 54-57, 59-64 are classified in Subgroup 2 as medium level of total efficiency. Lastly, data points1, 3-6, 8, 9, 11, 13-17, 20, 21 are classified in Subgroup 3 as high level of total efficiency. All these subgroups are tabulated in Table 4.

Table 4. Subgroups of training dataset with respect to the classification outcomes

Subgroup	Data point	Outcome
Subgroup 1	$23,\ 30,\ 43,\ 53,\ 58,\ 65-70$	Low
Subgroup 2	2, 7, 10, 12, 18, 19, 22, 24-29, 31-42, 44-52, 54-57, 59-4	Medium
Subgroup 3	1, 3-6, 8, 9, 11, 13-17, 20, 21	High

Step 4: Then, the fuzzy subsethood values of each linguistic term, tabulated in Table 5, are calculated using Equation (4). The fuzzy subsethood value A which is a subset of B is denoted by $S(B,\ A)$ where $S(B,\ A) \in [0,\ 1]$. Here, $S(B,\ A)$

refers to fuzzy subsethood value of fuzzy set A to fuzzy set B, $\mu_A(x)$ and $\mu_B(x)$ refer to membership value in x in set A and B, respectively.

$$S(B,\ A) = \frac{M(B,\ A)}{M(B)} = \frac{\sum_{x\in U} \nabla\left(\mu_B(x),\ \mu_A(x)\right)}{\sum_{x\in U} \mu_B(x)} \tag{4}$$

Table 5. Subsethood values

	Total efficiency		
Linguistic term	Low	Medium	High
A_1	0.5877	0.4700	0.0686
A_2	0.1741	0.4639	0.3017
A_3	0.4123	0.4341	0.6297
B_1	0.5482	0.1154	0.1509
B_2	0.4448	0.6136	0.7098
B_3	0.3371	0.6080	0.1393
C_1	0.0.9895	0.7130	0.0000
C_2	0.0641	0.6312	0.0451
C_3	0.0034	0.0286	0.9549

Step 5: Next, the weights of each linguistic term are calculated using the subsethood values. Equation (5) is used to compute the weights of the subsethood values for each linguistic term, which are tabulated in Table 6. In this context, the weights range from 0 to 1, where higher weights indicate greater importance, and lower weights indicate less importance.

$$W\left(X,\ A_i\right) = \frac{S\left(X,\ A_i\right)}{\max_{i=1,\ 2,\ \ldots,\ l} S\left(X,\ A_i\right)} \tag{5}$$

where $W\left(X,\ A_i\right) \in [0,\ 1]$ and $i = 1,\ 2,\ \ldots,\ l$.

Table 6. Weights for each linguistic term

	Total efficiency		
Linguistic term	Low	Medium	High
A_1	1.0000	1.0000	0.1089
A_2	0.2962	0.9869	0.4791
A_3	0.7017	0.9235	1.0000
B_1	1.0000	0.1881	0.2126
B_2	0.8114	1.0000	1.0000
B_3	0.6150	0.9910	0.1962
C_1	1.0000	1.0000	0.0000
C_2	0.0648	0.8853	0.0472
C_3	0.0034	0.0400	1.0000

The weights of each linguistic term are considered as quantifier "some" or "all". If the weight is equal to 1, then the quantifier is regarded to be "all". Otherwise, it is considered to represent "some". The weight of the respective linguistic term can be used to represent the extent to which "some" is interpreted. The concluding classification is made based on the rule with the highest overall weight.

Step 6: Next, the rules, generated based on the weight calculated in Step 5, are shown in Figure 4 below.

Rule 1:
If solar radiation is 1.0000 A_1 or 0.2962 A_2 or 0.7017 A_3,
And ambient temperature is 1.0000 B_1 or 0.8114 B_2 or 0.6150 B_3,
And air mass flowrate is 1.0000 C_1 or 0.0648 C_2 or 0.0034 C_3,
then total efficiency is low.
Rule 2:
If solar radiation is 1.0000 A_1 or 0.9869 A_2 or 0.9235 A_3,
And ambient temperature is 0.1881 B_1 or 1.0000 B_2 or 0.9910 B_3,
And air mass flowrate is 1.0000 C_1 or 0.8853 C_2 or 0.0400 C_3,
then total efficiency is medium.
Rule 3:
If solar radiation is 0.1089 A_1 or 0.4791 A_2 or 1.0000 A_3,
And ambient temperature is 0.2126 B_1 or 1.0000 B_2 or 0.1962 B_3,
And air mass flowrate is 0.0000 C_1 or 0.0472 C_2 or 1.0000 C_3,
then total efficiency is high.

Figure 4. Rule set generated

Step 7: Once the rule set is obtained, the classification of the output of PV/T solar collector performance can be carried out for all data points where three conditional attributes are obtained. The following example is provided to demonstrate how the output (total efficiency) is determined for each data point.

For example, given a set of data taken from the testing dataset where the value of radiation, A_i is 200 $\mathrm{W \cdot m^{-2}}$, ambient temperature, B_i is 302 K and air mass flowrate, C_i is 0.008225 $\mathrm{kg \cdot s^{-1}}$, where A_i, B_i and C_i, $i = 1,\ 2,\ 3$, refer to the linguistic. These values need to be transformed into fuzzy values, using fuzzy membership function shown in Table 1. Therefore, from the calculations, the transformed fuzzy values are as follows:

$$\begin{gathered}\mu_{A_1}(200) = 0.81981,\ \mu_{A_2}(200) = 0.18019,\ \mu_{A_3}(200) = 0 \\ \mu_{B_1}(302) = 1,\ \mu_{B_2}(307) = 0,\ \mu_{B_3}(307) = 0 \\ \mu_{C_1}(0.008225) = 1,\ \mu_{C_2}(0.008225) = 0,\ \mu_{C_3}(0.008225) = 0\end{gathered} \tag{6}$$

Next, the rules are computed using the generated rule set as shown in Figure 5 and the transformed values mentioned earlier. In this process, the Min-Max Operator is used. The highest truth value between the three rules will determine the level of total efficiency for the set of data.

Rule 1:

$$\begin{aligned}E_1 = \min\big[&\max\left(\mu_{A_1} \times A_1,\ \mu_{A_2} \times 0.2962A_2,\ \mu_{A_3} \times 0.7017A_3\right),\ \max\left(\mu_{B_1} \times B_1,\ \mu_{B_2} \times 0.8114B_2,\ \mu_{B_3}\right. \\ &\left.\times 0.6150B_3\right),\ \max\left(\mu_{C_1} \times C_1,\ \mu_{C_2} \times 0.0648C_2,\ \mu_{C_3} \times 0.0034C_3\right)\big] = 0.81981\end{aligned} \tag{7}$$

Rule 2:

$$E_2 = \min\left[\max\left(\mu_{A_1} \times A_1,\ \mu_{A_2} \times 0.9869A_2,\ \mu_{A_3} \times 0.9235A_3\right),\ \max\left(\mu_{B_1} \times 0.1881B_1,\ \mu_{B_2} \times B_2,\ \mu_{B_3} \times 0.9910B_3\right),\ \max\left(\mu_{C_1} \times C_1,\ \mu_{C_2} \times 0.8853C_2,\ \mu_{C_3} \times 0.0400C_3\right)\right] = 0.18814 \tag{8}$$

Rule 3:

$$E_3 = \min\left[\max\left(\mu_{A_1} \times 0.1089A_1,\ \mu_{A_2} \times 0.4791A_2,\ \mu_{A_3} \times A_3\right),\ \max\left(\mu_{B_1} \times 0.2126B_1,\ \mu_{B_2} \times B_2,\ \mu_{B_3} \times 0.1962B_3\right),\ \max\left(\mu_{C_2} \times 0.0472C_2,\ \mu_{C_3} \times C_3\right)\right] = 0 \tag{9}$$

Based on the truth values of each rule calculated, the highest truth value is associated with Rule 1. Hence, the classification result is E_1, indicating that the thermal efficiency is low. This aligns with the actual classification of the total efficiency in the original testing dataset, which is also low. Then, the remaining data in the testing dataset has also been classified into Low, Medium and High using the rules, which reveals that the predicted total efficiency is 81.25% similar to the original classification.

2.2 *Fuzzy subjective evaluation using similarity function*

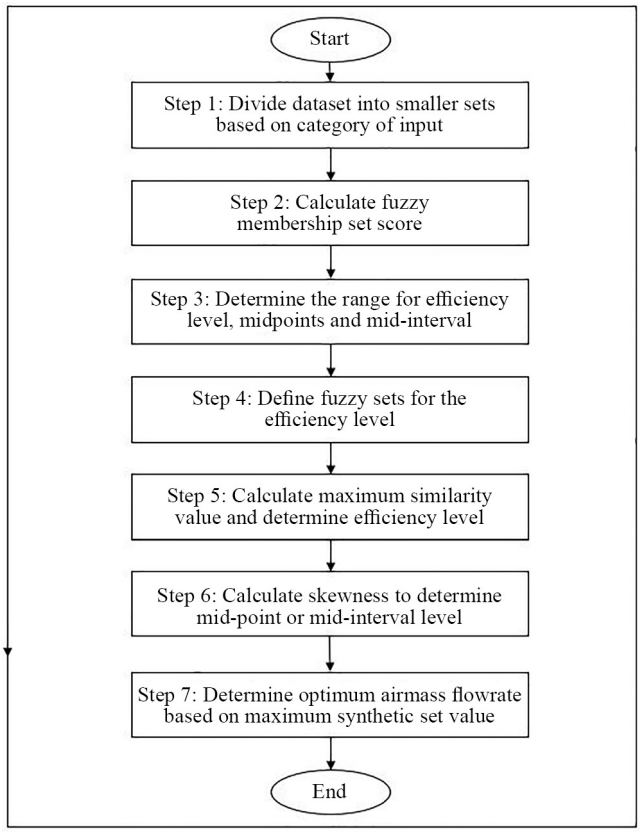

Figure 5. Flowchart for the proposed fuzzy subjective evaluation method

The fuzzy subjective evaluation method utilizes a dataset generated from fuzzy rules developed by the weighted subsethood-based algorithm. This dataset comprises the total efficiency levels of the PV/T solar collector under varying conditions of ambient temperature, solar radiation, and air mass flowrate. The subjective evaluation framework used in this study integrates methodologies from previous studies [16–19].

The algorithm for the fuzzy subjective evaluation using similarity function is illustrated in the flowchart in Figure 5.

Step 1: The determination of the optimum level of air mass flowrate started with the dataset being divided into nine sets, S_n, where $n = 1, 2, \ldots, 9$, based on the level of ambient temperature and solar radiation. For instance, "Set 1, (S_1)" represents efficiency data when the ambient temperature and solar radiation are at low level. Table 7 provides a detailed description.

Table 7. Sets of data categorized based on levels of ambient temperature and solar radiation

Ambient temperature level	Solar radiation level		
	Low	Medium	High
Low	Set 1 (S_1)	Set 2 (S_2)	Set 3 (S_3)
Medium	Set 4 (S_4)	Set 5 (S_5)	Set 6 (S_6)
High	Set 7 (S_7)	Set 8 (S_8)	Set 9 (S_9)

Table 8. Frequency of efficiency level for each set

Set	Efficiency level	Air mass flowrate		
		F_1	F_2	F_3
S_1	Low	17	8	12
	Medium	5	8	12
	High	1	0	0
S_2	Low	12	6	9
	Medium	1	6	6
	High	0	0	3
S_3	Low	20	0	0
	Medium	20	20	0
	High	0	20	59
S_4	Low	12	6	9
	Medium	0	6	6
	High	0	0	3
S_5	Low	16	8	12
	Medium	5	8	12
	High	5	0	0
S_6	Low	15	0	0
	Medium	15	15	0
	High	0	15	45
S_7	Low	21	1	1
	Medium	20	20	2
	High	1	20	59
S_8	Low	15	10	11
	Medium	15	26	12
	High	12	4	45
S_9	Low	13	11	10
	Medium	12	26	12
	High	12	5	44

Step 2: A frequency table (Table 8) is constructed to show the occurrence of efficiency levels for each set. The data are used to calculate the membership set score. In this context, F_i represents the fuzzy set membership of the subjective evaluation level, where $i = 1,\ 2,\ ...,\ n$ alternatives. $\mu_{(F_i)}(x)$ denotes the membership set score of alternatives according to criteria.

Table 9 depicts the membership set score of efficiency level, E_m, for all sets S_n at different level of air mass flowrate, F_i, where $m = 1,\ 2,\ 3$ and $i = 1,\ 2,\ 3$. The experimental dataset is transformed into membership set score using Equation (10), to generate generalised values between different variables.

$$\text{Membership set score } = \frac{F_i}{\sum_{i=1}^{3} F_i} \tag{10}$$

Based on Table 7, the frequency of the data in each set is calculated from the dataset and the membership set score for the combination as shown in Table 8. For example, the value 0.7391 for S_1 is obtained by dividing F_1 of E_1 with the total data $\sum_{m=1}^{3} F_{1,\,m}$ i.e.

$$\text{Membership set score } = \frac{F_1}{\sum_{i=1}^{3} F_i} = \frac{17}{17+5+1} = 0.7391 \tag{11}$$

Table 9. Membership set score for every set

Efficiency level	Mid-point/Mid-interval value (M)			
Set	Efficiency level	Air mass flowrate		
		F_1	F_2	F_3
S_1	E_1	0.7391	0.5000	0.5000
	E_2	0.2174	0.5000	0.5000
	E_3	0.0435	0.0000	0.0000
S_2	E_1	0.9231	0.5000	0.5000
	E_2	0.0769	0.5000	0.3333
	E_3	0.0000	0.0000	0.1667
S_3	E_1	0.5000	0.0000	0.0000
	E_2	0.5000	0.5000	0.0000
	E_3	0.0000	0.5000	1.0000
S_4	E_1	1.0000	0.5000	0.5000
	E_2	0.0000	0.5000	0.3333
	E_3	0.0000	0.0000	0.1667
S_5	E_1	0.6154	0.5000	0.5000
	E_2	0.1923	0.5000	0.5000
	E_3	0.1923	0.0000	0.0000
S_6	E_1	0.5000	0.0000	0.0000
	E_2	0.5000	0.5000	0.0000
	E_3	0.0000	0.5000	1.0000
S_7	E_1	0.5000	0.0244	0.0161
	E_2	0.4762	0.4878	0.0323
	E_3	0.0238	0.4878	0.9516
S_8	E_1	0.3571	0.2500	0.1618
	E_2	0.3571	0.6500	0.1765
	E_3	0.2857	0.1000	0.6618
S_9	E_1	0.3514	0.2619	0.1515
	E_2	0.3243	0.6190	0.1818
	E_3	0.3243	0.1190	0.6667

Step 3: The mid-point and mid-interval values of efficiency are then determined from the range of efficiency values, $[x_{\min},\ x_{\max}]$ where $x_{\min}$ and $x_{\max}$ represent the lowest and highest value of efficiency obtained from the experimental data, respectively. The mid-point and mid-interval values are used in categorizing each criterion. The mid-point is determined using Equation (12).

$$\text{midpoint} = \frac{x_{\min} + x_{\max}}{2} \tag{12}$$

Mid-intervals, consisting of four equal intervals of each efficiency level range, are calculated using Equations (13) and (14).

$$\text{first quarter of mid} - \text{interval} = \frac{x_{\min} + x_{\max}}{4} \tag{13}$$

$$\text{third quarter of mid} - \text{interval} = \frac{3\,(x_{\min} + x_{\max})}{4} \tag{14}$$

The range, mid-point and mid-interval values for all efficiency levels are illustrated in Table 10.

Table 10. Mid-point and mid-interval for each efficiency level

Efficiency level	Mid-point/Mid-interval value (M)				
Low	0.1046	0.1345	0.1645	0.1945	0.2244
Medium	0.2244	0.2653	0.3063	0.3472	0.3881
High	0.3881	0.4268	0.4655	0.5042	0.5429

Step 4: The construction of fuzzy sets level is defined in Table 11, which is adopted from the work done in [16].

Table 11. Fuzzy set for efficiency level

Efficiency level	Linguistic variable	Fuzzy set
Low	Unsatisfactory	{0.1, 0.9, 0.2}
Medium	Satisfactory	{0.4, 0.4, 0}
High	Good	{1.0, 0.2, 0}

Step 5: The maximum similarity value is then calculated using fuzzy similarity function. This function is used to define the degree of similarity between the standard fuzzy set levels Low, Medium and High and the fuzzy value of each criterion. The defined efficiency level is the process of mapping the fuzzy value of the criteria to the similarity value, $S(F,\ M)$, which is calculated using Equation (15).

$$S(F,\ M) = \frac{\hat{F} \cdot \hat{M}}{\max(\hat{F} \cdot \hat{F},\ \hat{M} \cdot \hat{M})} \tag{15}$$

where $\hat{F} = (\mu_F(x_1),\ \mu_F(x_2),\ \ldots,\ )$ and $\hat{M} = (\mu_M(x_1),\ \mu_M(x_2),\ \ldots,)$ are vectors. Here, $\hat{M}$ denotes the transpose vectors Low ^{T}, Medium ^{T} and High ^{T}, and $\widehat{F}$ denotes the transpose vector of fuzzy set F_i. The set $X = (x_1,\ x_2,\ \ldots,\ x_n)$ represents the set of universe discourse, and the symbol "." represents the dot product operator. Then, the maximum similarity value is determined by identifying the largest similarity values for every level of each criterion.

The similarity values for each criterion across all sets are calculated first and presented in Table 12. The values in the table indicate the similarity between the criterion, which represent the level of air mass flowrate, F_i, for $i = 1,\ 2,\ 3$ and the efficiency level for each set.

Table 12. Similarity value

Set	Efficiency level	Air mass flowrate		
		F_1	F_2	F_3
S_1	E_1	0.5100	0.5135	0.5135
	E_2	0.6425	0.8000	0.8000
	E_3	0.7525	0.5769	0.5769
S_2	E_1	0.5364	0.5135	0.4505
	E_2	0.4662	0.8000	0.8571
	E_3	0.9024	0.5769	0.5449
S_3	E_1	0.5135	0.2973	0.1081
	E_2	0.8000	0.4000	0.0000
	E_3	0.5769	0.0962	0.0000
S_4	E_1	0.5405	0.5135	0.4505
	E_2	0.4000	0.8000	0.8571
	E_3	0.9615	0.5769	0.5449
S_5	E_1	0.4470	0.5135	0.5135
	E_2	0.7137	0.8000	0.8000
	E_3	0.2811	0.0000	0.0000
S_6	E_1	0.5135	0.2973	0.1081
	E_2	0.8000	0.4000	0.0000
	E_3	0.5769	0.0962	0.0000
S_7	E_1	0.5045	0.3032	0.1273
	E_2	0.8181	0.4300	0.0213
	E_3	0.5723	0.1173	0.0217
S_8	E_1	0.3977	0.4622	0.2448
	E_2	0.8485	0.7273	0.2732
	E_3	0.4121	0.3654	0.1895
S_9	E_1	0.3828	0.4556	0.2424
	E_2	0.8096	0.7562	0.2664
	E_3	0.4002	0.3709	0.1807

The maximum similarity value for each criterion is identified from the highest similarity values, as shown in the third column of Table 13, and the efficiency level is then determined. The skewness value of the maximum similarity values in each set is calculated and shown in the fourth column of Table 13. The efficiency level is then mapped to the appropriate mid-point and mid-interval value to determine the synthetic score value.

Table 13. Maximum similarity value

Set	Air mass flowrate	Max similarity value	Skewness value	Efficiency level	Synthetic score value
	F_1	0.7525	1.65	E_1	0.1345
S_1	F_2	0.8000	1.39	E_1	0.1345
	F_3	0.8000	1.39	E_1	0.1345
	F_1	0.9024	1.56	E_1	0.1345
S_2	F_2	0.8000	1.39	E_1	0.1345
	F_3	0.8571	1.36	E_1	0.1345
	F_1	0.8000	1.39	E_2	0.2653
S_3	F_2	0.4000	−0.91	E_2	0.3472
	F_3	0.1081	1.73	E_2	0.2653
	F_1	0.9615	1.29	E_1	0.1345
S_4	F_2	0.8000	1.39	E_1	0.1345
	F_3	0.8571	1.36	E_1	0.1345
	F_1	0.7137	1.57	E_1	0.1345
S_5	F_2	0.8000	−1.09	E_1	0.1945
	F_3	0.8000	−1.18	E_1	0.1945
	F_1	0.8000	1.39	E_2	0.2653
S_6	F_2	0.4000	−0.91	E_2	0.3472
	F_3	0.1081	1.73	E_2	0.2653
	F_1	0.8181	1.41	E_2	0.2653
S_7	F_2	0.4300	−0.56	E_2	0.3472
	F_3	0.1273	1.73	E_2	0.2653
	F_1	0.8485	1.73	E_2	0.2653
S_8	F_2	0.7273	1.23	E_2	0.2653
	F_3	0.2732	−0.91	E_2	0.3472
	F_1	0.8096	1.72	E_2	0.2653
S_9	F_2	0.7562	1.40	E_2	0.2653
	F_3	0.2664	−1.18	E_2	0.3472

Step 6: Lastly, the maximum synthetic score value and the optimum air mass flowrate for each set are determined, as tabulated in Table 14. From these results, the selection of optimum air mass flowrate for different levels of ambient temperature and solar radiation is identified and is shown in Table 15.

Table 14. Maximum synthetic score value

Set	Maximum synthetic score value	Optimum air mass flowrate
S_1	0.1345	F_1
S_2	0.1345	F_1
S_3	0.3472	F_2
S_4	0.1345	F_1
S_5	0.1945	F_2
S_6	0.3472	F_2
S_7	0.3472	F_2
S_8	0.3472	F_3
S_9	0.3472	F_3

Table 15. Optimum air mass flow rate for different levels of ambient temperature and solar radiation

Ambient temperature level	Solar radiation level		
	Low	Medium	High
Low	F_1	F_1	F_2
Medium	F_1	F_2	F_3
High	F_2	F_3	F_3

2.3 *Validation of method using sensitivity analysis*

In this study, sensitivity analysis is used to validate the results obtained from the integration of Weighted Subsethood-based algorithm and Fuzzy Subjective Evaluation. The value of medium level membership functions of input variables; solar radiation and ambient temperature; and the output temperature are used in the sensitivity analysis. The medium value of solar radiation is 371.875 $W \cdot m^{-2}$ and 306.013 K for ambient temperature. The values are then normalised to determine the significance of changes of each input parameter on the total efficiency, using the formula $x_{\text{norm}} = \dfrac{x - x_{\min}}{\text{range of } x}$, where range of $x = x_{\max} - x_{\min}$, as shown in Table 16. Then, the sensitivity analysis was carried out by varying the changes of the input parameters by increasing and decreasing by 5% and 10% to observe the impact on the total efficiency.

Table 16. Normalised value for medium membership function of solar radiation and ambient temperature

	Solar radiation	Ambient temperature
Minimum value, $x_{\min}$	100	301
Medium value x_{med}	371.875	306.013
Maximum value, $x_{\max}$	1,000	312
Normalized medium value, x_{norm}	$x_{\text{norm}} = \dfrac{371.875 - 100}{1,000 - 100}$	$x_{\text{norm}} = \dfrac{306.013 - 301}{312 - 301}$
	$x_{\text{norm}} = 0.30208$	$x_{\text{norm}} = 0.01612$

The normalised values for solar radiation and ambient temperature have been utilized to determine the increased and decreased values of the actual value of the input parameters as shown in Table 17.

Table 17. The normalised and actual values of solar radiation and ambient temperature for each percentage change

Changes in input parameter	Solar radiation		Ambient temperature	
	x_{norm}	Actual value ($\text{W} \cdot \text{m}^{-2}$)	x_{norm}	Actual value (K)
$x_{\text{norm}} - 5\%$	0.27186	344.6713	0.41016	305.5117
$x_{\text{norm}} - 10\%$	0.28696	358.2642	0.43294	305.7642
Normalised medium value, x_{norm}	0.30208	371.857	0.45573	306.013
$x_{\text{norm}} + 5\%$	0.31717	385.4499	0.47851	306.2637
$x_{\text{norm}} + 10\%$	0.33227	399.0427	0.50130	306.5143

In Table 18, the effect of percentage change in solar radiation with fixed ambient temperature on total efficiency are shown in terms of normalised values and actual values. When solar radiation is reduced by 5% and 10%, the total efficiency is reduced by 2.994% and 1.393%, respectively. Meanwhile, when the solar radiation increases by 5% and 10%, the total efficiency is increased by 1.323% and 2.507%, respectively.

Table 18. The effect of percentage change in solar radiation with fixed ambient temperature on total efficiency in terms of normalised values and actual values

	Solar radiation	Ambient temperature	Total efficiency	Normalised total efficiency	% Change of total efficiency
$x_{\text{norm}} - 5\%$	344.6713	306.013	0.3203	0.561694	−2.994
$x_{\text{norm}} - 10\%$	358.2642	306.013	0.3226	0.570968	−1.393
Normalised medium value, x_{norm}	371.857	306.013	0.3246	0.579032	0
$x_{\text{norm}} + 5\%$	385.4499	306.013	0.3265	0.586694	1.323
$x_{\text{norm}} + 10\%$	399.0427	306.013	0.3282	0.593548	2.507

In Table 19, the effect of percentage change in ambient temperature with fixed solar radiation on total efficiency are shown in terms of normalised values and actual values. When ambient temperature is reduced by 5% and 10%, the total efficiency is reduced by 0.348% and 0.209%, respectively. Meanwhile, when ambient temperature is increased by 5% and 10%, the total efficiency is increased by 0.209% and 0.348%, respectively.

Table 19. The effect of percentage change in ambient temperature with fixed solar radiation on total efficiency in terms of normalised values and actual values

	Solar radiation	Ambient temperature	Total efficiency	Normalised total efficiency	% Change of total efficiency
$x_{\text{norm}} - 5\%$	371.857	305.5117	0.3241	0.577016	−0.348
$x_{\text{norm}} - 10\%$	371.857	305.7624	0.3243	0.577823	−0.209
Normalised medium value, x_{norm}	371.857	306.013	0.3246	0.579032	0
$x_{\text{norm}} + 5\%$	371.857	306.2637	0.3249	0.580242	−0.209
$x_{\text{norm}} + 10\%$	371.857	306.5143	0.3251	0.581048	−0.348

Based on the results of the sensitivity analysis above, it can be concluded that the solar collector system is more sensitive towards changes in solar radiation, compared to ambient temperature. Since solar collectors operate to harvest solar energy, it has been proven that the model developed can be used to perform the analysis of the solar collector system.

3. Results and discussion

In this study, the fuzzy rules for the performance of PV/T solar collector have been generated. The fuzzy rules can be used to predict the performance of the collector under changes of surrounding conditions. Then, the fuzzy subjective evaluation using similarity function has been carried out on the dataset to determine the optimum air mass flowrate for every possible weather condition to ensure optimum efficiency of the solar collector. Lastly, sensitivity analysis has been performed to observe the effect of changes of solar radiation and ambient temperature on the total efficiency of the solar collector.

Based on the results obtained; to maintain an optimal performance of the PV/T solar collector, the air mass flowrate needs to be adjusted according to the current surrounding temperature as follows:

i. When the ambient temperature and solar radiation are low or medium, the optimum air mass flow rate is low.

ii. When the ambient temperature is low and solar radiation is high, the optimum air mass flow rate is medium.

iii. When the ambient temperature is medium and solar radiation is low, the optimum air mass flow rate is low.

iv. When the ambient temperature is medium and solar radiation is medium or high, the optimum air mass flow rate is medium.

v. When the ambient temperature is high and solar radiation is low, the optimum air mass flow rate is medium.

vi. When the ambient temperature is high and solar radiation is medium or high, the optimum air mass flow rate is high.

These findings demonstrate that the highest air mass flowrate is not always necessary under varying surrounding conditions. Selecting the optimum air mass flowrate can help maintain the balance between the input and output energy of the PV/T solar collector.

4. Conclusions

This study demonstrates the method to optimise the performance of an air-based Photovoltaic/Thermal (PV/T) solar collector by integrating fuzzy logic with weighted subsethood-based algorithm. The research presents an effective adaptive control system that can react automatically to changing environmental conditions, improving the system's electrical and thermal efficiency by overcoming the drawbacks of human control and simple automation. The main conclusions show that incorporating a fuzzy subjective evaluation method greatly lowers decision-making inconsistencies and guarantees ideal operational conditions under a range of environmental factors. Furthermore, the created fuzzy rule-based system efficiently adapts to variations in wind speed, ambient temperature, and sun radiation to estimate the optimal air mass flowrate in real-time.

The findings also show that the maximum fan speed is only required in situations with medium to high levels of solar radiation and ambient temperature, which lowers energy use in less taxing circumstances. Additionally, choosing the ideal air mass flowrate maximises system efficiency by preserving equilibrium between the solar collector's input and output energies.

This work is important because it advances solar energy technology by offering a more flexible, accurate, and effective method of controlling energy conversion in PV/T systems. The constantly changing and irregular nature of environmental influences can often be a challenge for traditional management approaches to handle, resulting in inadequate performance. This study addresses a significant void in the optimisation of air-based PV/T systems by automating the control procedure and utilising fuzzy logic's advantages. The proposed system not only improves energy efficiency but also reduces operational complexity, making it a promising candidate for widespread adoption in residential, commercial, and industrial applications.

Additionally, this work emphasises how fuzzy logic-based control systems might revolutionise the optimisation of air-based PV/T solar collectors. The system will function at its best under a variety of circumstances thanks to its capacity to dynamically modify air mass flowrates in response to real-time environmental data. This flexibility is especially crucial in areas with extremely fluctuating weather patterns, where conventional management techniques frequently prove

ineffective. The research helps the world move towards a more sustainable and energy-efficient future by tackling these issues and opening the door for more dependable and sustainable renewable energy alternatives.

5. Recommendations

To further advance this research, the following recommendations are proposed. First, a comparative analysis with existing solar collector systems should be conducted to showcase the advantages and unique features of the proposed compact air PV/T solar collector in terms of performance, efficiency, and cost-effectiveness. Additionally, a long-term performance evaluation is necessary to assess the system's stability, durability, and energy output over time, addressing reliability challenges in varying weather conditions. The fuzzy optimization methodology used to determine optimal operating conditions could also be refined through sensitivity analysis, testing the algorithm's performance under various scenarios. By pursuing these research directions, future studies can build upon the current findings and further improve the efficiency and applicability of PV/T solar collector systems.

Acknowledgement

This research is supported with fundings and facilities by Universiti Kuala Lumpur and Yayasan Universiti Teknologi PETRONAS. The author would also like to convey their gratitude to the reviewers for the helpful remarks and suggestions for this paper.

Conflict of interest

The authors declare no competing financial interest.

References

[1] *Full report-Statistical Review of World Energy 2021*. UK: British Petroleum. 2021. Available from: https://www.bp.com/content/dam/bp/business-sites/en/global/corporate/pdfs/energy-economics/statistical-review/bp-stats-review-2021-full-report.pdf.

[2] Sharma A, Tyagi VV, Chen CR, Buddhi D. Review on thermal energy storage with phase change materials and applications. *Renewable and Sustainable Energy Reviews*. 2009; 13(2): 318-345. Available from: https://doi.org/10.1016/j.rser.2007.10.005.

[3] Hasnain SM. Review on sustainable thermal energy storage technologies, part I: Heat storage materials and techniques. *Energy Conversion and Management*. 1998; 39(11): 1127-1138. Available from: https://doi.org/10.1016/S0196-8904(98)00025-9.

[4] Pardo P, Deydier A, Anxionnaz-Minvielle Z, Rougé S, Cabassud M, Cognet P. A review on high temperature thermochemical heat energy storage. *Renewable and Sustainable Energy Reviews*. 2014; 32: 591-610. Available from: https://doi.org/10.1016/j.rser.2013.12.014.

[5] Khudhair AM, Farid M. A review on energy conservation in building applications with thermal storage by latent heat using phase change materials. *Energy Conversion and Management*. 2004; 45(2): 263-275. Available from: https://doi.org/10.1016/S0196-8904(03)00131-6.

[6] Zhou C, Liang R, Zhang J. Optimization design method and experimental validation of a solar pvt cogeneration system based on building energy demand. *Energies*. 2017; 10(9): 1281. Available from: https://doi.org/10.3390/en10091281.

[7] Tonui JK, Tripanagnostopoulos Y. Air-cooled PV/T solar collectors with low cost performance improvements. *Solar Energy*. 2007; 81(4): 498-511. Available from: https://doi.org/10.1016/j.solener.2006.08.002.

[8] Othman MY, Yatim B, Sopian K, Bakar MNA. Performance analysis of a double-pass photovoltaic/thermal (PV/T) solar collector with CPC and fins. *Renewable Energy*. 2005; 30(13): 2005-2017. Available from: https://doi.org/10.1016/j.renene.2004.10.007.

[9] He W, Chow TT, Ji J, Lu J, Pei G, Chan LS. Hybrid photovoltaic and thermal solar-collector designed for natural circulation of water. *Applied Energy*. 2006; 83: 199-210.

[10] Bambrook SM, Sproul AB. Maximising the energy output of a PVT air system. *Solar Energy*. 2012; 86(3): 1857-1871. Available from: https://doi.org/10.1016/j.apenergy.2005.02.007.

[11] Agrawal B, Tiwari GN. *Building Integrated Photovoltaic Thermal Systems: For Sustainable Developments*. UK: Royal Society of Chemistry; 2011.

[12] Yager RR, Zadeh LA. *An Introduction to Fuzzy Logic Applications in Intelligent Systems*. New York: Springer; 1992. Available from: https://doi.org/10.1007/978-1-4615-3640-6.

[13] Rahim NF, Othman M, Sokkalingam R, Kadir EA. Forecasting crude palm oil prices using fuzzy rule-based time series method. *IEEE Access*. 2018; 6: 32216-32224. Available from: https://doi.org/10.1109/ACCESS.2018.2846809.

[14] Izquierdo SS, Izquierdo LR. Mamdani fuzzy systems for modelling and simulation: A critical assessment. *Journal of Artificial Societies and Social Simulation*. 2018; 21(3): 2. Available from: https://doi.org/10.18564/jasss.3660.

[15] Rasmani KA, Shen Q. Data-driven fuzzy rule generation and its application for student academic performance evaluation. *Applied Intelligence*. 2006; 25: 305-319. Available from: https://doi.org/10.1007/s10489-006-0109-9.

[16] Biswas R. An application of fuzzy sets in students' evaluation. *Fuzzy Sets and Systems*. 1995; 74(2): 187-194. Available from: https://doi.org/10.1016/0165-0114(95)00063-Q.

[17] Chu F. Quantitative evaluation of university teaching quality-an application of fuzzy set and approximate reasoning. *Fuzzy Sets and Systems*. 1990; 37(1): 1-11. Available from: https://doi.org/10.1016/0165-0114(90)90058-E.

[18] Othman M, Ku-Mahamud KR. Fuzzy multi criteria evaluation for performance of bus companies. *Computer and Information Science*. 2010; 3(2): 252-252. Available from: https://doi.org/10.5539/cis.v3n2p252.

[19] Othman M, Ku-Mahamud KR, Bakar AA. Fuzzy evaluation method using fuzzy rule approach in multicriteria analysis. *Yugoslav Journal of Operations Research*. 2008; 18(1): 95-107. Available from: https://doi.org/10.2298/YJOR0801095O.